NJC

PAPER

View Article Online
View Journal | View Issue

Cite this: *New J. Chem.*, 2015, **39**, 9207

How the stereochemistry decides the selectivity: an approach towards metal ion detection†

Manas Kumar Bera, Chanchal Chakraborty and Sudip Malik*

Received (in Montpellier, France) 6th May 2015,
Accepted 7th September 2015

DOI: 10.1039/c5nj01148e

www.rsc.org/njc

The stereochemistry of the coordination sites of a ligand plays a specific role in its binding with metals in a specific geometry. Herein, we designed and successfully prepared three different fluorene-based $(A-B)_n$-type salen polymers (achiral **FSP1**, **FSP2**, and chiral **FSP3**), wherein the A-part is fluorophore and the B-part is the receptor. In the receptor, the coordination sites have four atoms (ONNO) that can bind any metal ion, but the orientation of ONNO differs in the three polymers. This orientation of the coordination site (*i.e.*, the stereochemistry) into the receptor part of the polymer makes them more selective for a particular metal ion. In this study, it is shown that the orientation of the coordination sites of the receptor in the main chain polymer significantly determines the selective detection behavior for metal ions. Among the three polymers, **FSP1** and **FSP2** are sensitive towards different metal ions but are not selective towards any particular metal ion. However, in contrast, **FSP3** is highly sensitive and selective to Zn^{2+} ions over other metal ions with a turn-on visible bright blue fluorescent color. This turn-on detection of the polymer is possibly due to the suppression of photo-induced electron transfer (PET) upon binding with Zn^{2+} ions. Theoretical calculations were also performed to show the orientation of the coordination sites. In **FSP3**, the coordination sites orient in a distorted tetrahedral fashion, which is very much prone to bind Zn^{2+} in a nearly tetrahedral geometry and that makes it more selective for Zn^{2+} ions only. The coordination geometry was also supported by 2D NMR studies. This report provides a template for the suitable design of a Zn^{2+} sensor, depending on the nature of the receptor incorporated into the main chain polymer.

Introduction

To obtain guidance for the development of a new sensor technology, one should just follow nature. The ultimate chemical sensors have already been developed by living organisms. For instance, some insects can detect chemical signals with perfect specificity and implausible sensitivity, whereas mammalian olfaction is based on an arrangement of less discriminating sensors and a memorized response pattern to recognize a unique odor. Such performance by biological systems is derived from a completely interactive system, where the receptor is served by analyte delivery and removal mechanisms. Selectivity comes from receptors and sensitivity is the outcome of analyte-triggered biochemical cascades. Any optimal artificial sensor system should ideally follow the above two features.

Recently, a widely explored field for metal ion detection is based on fluorescent sensors, because of their low cost, easy signal detection, high sensitivity, and selectivity. A typical fluorescent sensor should fulfill two basic criteria. First, binding selectivity, *i.e.*, the receptor must show strong affinity for a particular analyte or ion. Second, signal selectivity, *i.e.*, the environment will not disturb the fluorescence signal. Thus, the design of a fluorescence sensor depends on the recognition site (receptor) and the signal source (the fluorophore that will transform the recognition phenomena into a fluorescence signal).[1,2]

An interesting class of organic compound called a Schiff base is named in honor of Hugo Schiff, who first reported these compounds back in 1864.[3,4] Schiff-base compounds are simply prepared by condensing a carbonyl compound with an amine refluxed in alcohol.[5] If salicyl aldehyde or its derivative as a carbonyl group is condensed with diamine as amine, the resulting compound is called a salen, which is one of the most popular classes of ligands in coordination chemistry. They form stable complexes with metal ions through coordination by a tetradentate (ONNO) donor site.[6] However, their metal ion binding behavior depends on the spatial orientation of the donor site, as each metal ion is coordinated in a specific geometry. Some metal ions have the tendency to form a square-planar complex (*e.g.*, Cu^{2+}),[7] while some have a tendency to form a tetrahedral complex (Zn^{2+}).[8] Therefore, the orientation of the coordination site is crucial. If the geometry of the

Polymer Science Unit, Indian Association for the Cultivation of Science, 2A & 2B Raja S. C. Mullick Road, Jadavpur, Kolkata – 700032, India. E-mail: psusm2@iacs.res.in

† Electronic supplementary information (ESI) available: Details of NMR study, MALDI Spectra, spectral data, absorbance, fluorescence, computational details and 2D NMR studies. See DOI: 10.1039/c5nj01148e

coordination site matches with that of the metal ion, one may expect the selectivity toward a particular metal ion. If the geometries of both components (coordination site and metal ion) mismatch, there will be no selectivity, in spite of the sensitivity toward the metal ion.

Keeping all these facts in mind, we designed three different $(A–B)_n$-type salen polymers (**FSP1**, **FSP2**, and **FSP3**) in such a way that these three polymers provide a tetradentate (ONNO) donor site for metal ion binding. In $(A–B)_n$ polymer, the A-part is a fluorophore based on the fluorene moiety and the B-part is the receptor with four donor (ONNO) coordination sites. However, the orientation of the four donor coordination sites (ONNO) is different in the receptor part of the three synthesized polymers. All the polymers were successfully prepared by condensing the fluorene-based salicyladehyde (FSal)[9] with corresponding diamines (Scheme 1). Among these, two polymers (**FSP1** and **FSP2**) were achiral and one (**FSP3**) was chiral. Another interesting thing is that the structures of the diamines were different in the three polymers and so there should not be a similar orientation of the four coordinating atoms (ONNO) in each polymer. As a result, we expected the binding ability of the polymer to metal ions to be different. Surprisingly, **FSP3** was highly selective and sensitive only for Zn^{2+} ions. The orientation of the coordinating donor atoms of **FSP3** made it the most selective fluorescence sensor for Zn^{2+} ions, which play an important role in the human body. For example, several diseases such as Alzheimer's disease,[10,11] prostate cancer,[12] and diabetes[13] are associated with Zn^{2+} ions. Owing to the closed-shell $3d^{10}$ configuration of zinc, there is no optical spectroscopic signature of Zn^{2+} ion and this is a limitation of the detection method for Zn^{2+} ions. Therefore, the detection of Zn^{2+} ions is a growing interest in chemical and biological science. A number of fluorescence sensors based on fluorescein,[14] quinoline,[15,16] and peptides[17] for Zn^{2+} detection have been reported in the literature, though most of them are small molecular receptors. Polymer-based reports are scarcely seen.[18,19] The advantage of polymer-based over small molecules lies in the signal amplification, due to electronic communication into the polymer backbone, as suggested by Swager and co-workers.[20,21] As a result of this, conjugated polymers offer an enhanced optical response toward analytes over their monomer counterparts.

In addition, most of the reported Zn^{2+} sensors are unable to distinguish Zn^{2+} and Cd^{2+}, as Cd^{2+} belongs to the same group of the periodic table. In this context, it was a challenge for us to design a unique polymeric system which could detect Zn^{2+} from aqueous solution without the sensor being affected by other metal ions. Some reported salen-based polymers made of substituted benzene,[22] isoquinoline,[23] binaphthol,[24] and perylene[25] have been used for Zn^{2+} and Hg^{2+} sensors based on turn-on fluorescence through a suppressed photo-induced-electron-transfer (PET) mechanism. Apart from this PET mechanism, the spatial orientation of the four atoms of the coordination site of each salen unit plays a key role in the selective detection of metal ions, though there is no report about how the orientation of coordination site of any ligand determines metal ion selectivity. To the best of our knowledge, this is the first report where fluorene-based salen polymers have been used for the turn-on detection of Zn^{2+} ions using a new concept where the orientation of the coordination site determines metal ion selectivity, apart from the PET mechanism.

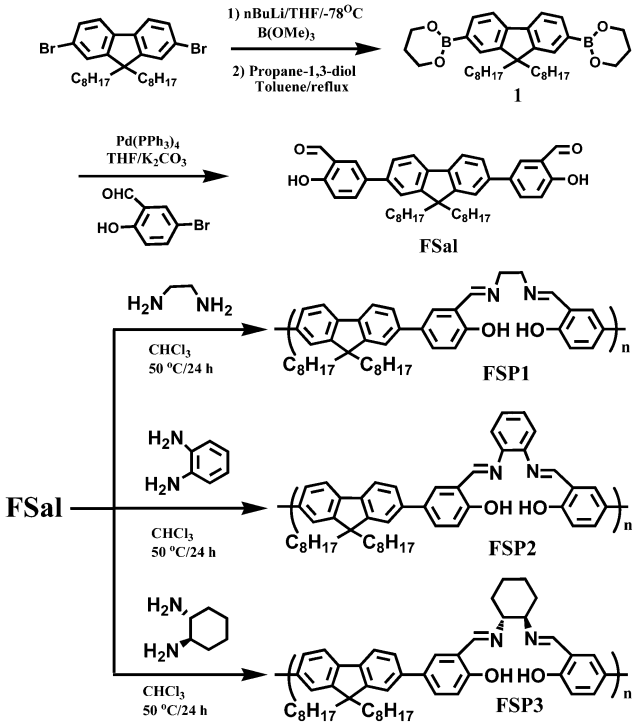

Scheme 1 Synthesis of three stereo chemically different salen-based polymers **FSP1**, **FSP2**, and **FSP3**.

Experimental section

Materials

Commercial grade reagents (2,7-dibromo-9,9-dioctylfluorene, 5-bromosalicylaldehyde, *n*-butyllithium (*n*-BuLi), tri-methylborate, 1,3-propanediol, tetrakis (triphenylphosphine) palladium(0) $[Pd(PPh_3)_4]$, ethylenediamine, *o*-phenylenediamine, and (1*R*,2*R*)-1,2-diaminocyclohexane from Sigma-Aldrich Co. Ltd and the rest from Merck India Pvt. Ltd) were used without further purification, and all the experiments were performed at room temperature (25 °C). All solvents used for the synthesis purpose were from Merck India Pvt. Ltd and distilled under a N_2 environment. For the spectroscopic measurements, HPLC grade tetrahydrofuran (THF) solvent was used, whereas double distilled H_2O was used to prepare the salt solutions. FSal was synthesized according to the previous report.[9]

Instruments

Fluorene-based salen polymers were characterized by ^{1}H-NMR, ^{13}C-NMR, and MALDI-TOF techniques. NMR spectra were acquired on a 500 MHz Bruker DPX spectrometer using $CDCl_3$ as the solvent and TMS as the standard reference at room temperature, with the chemical shift given in parts per million (ppm). UV-Vis spectra of all the samples were studied with a Hewlett–Packard UV-Vis spectrophotometer (model 8453). Emission studies of

the solution were performed with a Horiba Jobin Yvon Fluoromax 3 spectrometer at an excitation wavelength of 360 nm using slits 5/5. Thermogravimetric analysis (TGA) was done with a TA thermal analysis system at a heating rate of 10 °C min^{-1} under a N_2 environment. The FT-IR spectra were recorded in an FTIR-8400S instrument (Shimadzu) using the pellets of the samples diluted with KBr. Matrix-assisted laser desorption ionization time-of-flight (MALDI-TOF) mass spectrometry was done with a Bruker Ultra flextreme (Bruker Daltonics Pvt. Ltd) and diathranol was used as a matrix. The circular dichroism (CD) spectra of all the samples were taken in a spectropolarimeter (JASCO, model J-815) in a 1 mm quartz cuvette.

Computational details

All the electronic structure calculations were carried out using the Gaussian 09 suite from a quantum chemistry program. Density functional theory (DFT) calculations[26] and geometry optimization was performed at the B3LYP/6-31 G(d) level[27,28] and the optimized geometries were considered for single-point time-dependent DFT (TD-DFT) calculations at the B3LYP/TZVP level.[29]

Synthesis of FSP1

A mixture of FSal (100 mg, 0.16 mmol) and ethylenediamine (10 mg, 0.16 mmol) was dissolved in 6 mL of chloroform. The obtained solution was stirred at 50 °C for 24 h, cooled to room temperature, poured into 20 mL methanol, and stirred for half an hour to obtain the solid yellow polymer (88 mg, 80%).

^{1}H-NMR (500 MHz, $CDCl_3$): δ (ppm) 13.28 (s, 2H), 8.52 (s, 2H), 7.70–7.73 (d, 2H), 7.60–7.64 (dd, 2H), 7.47–7.54 (m, 6H), 7.04–7.07 (d, 2H), 4.03 (s, 4H), 2.01 (s, 4H), 0.69–1.25 (m, 30H). ^{13}C-NMR (500 MHz, $CDCl_3$): δ (ppm) 166.7, 160.6, 151.8, 139.8, 139.2, 132.7, 131.4, 130.0, 125.6, 121.0, 120.0, 118.9, 117.6, 60.1, 55.4, 40.6, 31.9, 30.1, 29.8, 29.3, 23.9, 22.7, 14.1. FT-IR: 1634 cm^{-1} (C═N), 3435 cm^{-1} (–OH).

Synthesis of FSP2

A mixture of FSal (100 mg, 0.16 mmol) and *o*-phenylenediamine (17.3 mg, 0.16 mmol) was dissolved in 6 mL of chloroform. The obtained solution was stirred at 50 °C for 24 h, cooled to room temperature, poured into 20 mL methanol, and stirred for half an hour to obtain the solid yellow polymer (90 mg, 77%).

^{1}H-NMR (500 MHz, $CDCl_3$): δ (ppm) 13.14 (s, 2H), 8.80 (s, 2H), 7.70–7.84 (m, 6H), 7.52–7.55 (m, 4H), 7.31–7.38 (d, 4H), 7.18–7.20 (d, 2H), 2.04 (s, 4H), 0.75–1.25 (m, 30H). ^{13}C-NMR (500 MHz, $CDCl_3$): δ (ppm) 163.8, 160.9, 151.8, 142.7, 139.8, 139.1, 132.5, 130.8, 128.4, 128.0, 125.6, 121.0, 120.1, 119.7, 118.2, 55.4, 40.6, 31.9, 30.1, 29.8, 29.3, 23.9, 22.7, 14.1. FT-IR: 1620 cm^{-1} (C═N), 3391 cm^{-1} (–OH).

Synthesis of FSP3

A mixture of FSal (100 mg, 0.16 mmol) and (*R*,*R*)-1,2-diaminocyclohexane (18.2 mg, 0.16 mmol) was dissolved in 6 mL of chloroform. The obtained solution was stirred at 50 °C for 24 h and then cooled to room temperature. The solution was poured into 20 ml methanol and stirred for 30 min to obtain the solid yellow polymer (92 mg, 78%).

^{1}H-NMR (500 MHz, $CDCl_3$): δ (ppm) 13.38 (s, 2H), 8.43 (s, 2H), 7.62–7.73 (m, 4H), 7.38–7.57 (m, 6H), 6.98–7.00 (d, 2H), 3.42 (m, 2H), 1.99 (m, 8H), 1.79 (m, 4H), 0.66–1.15 (m, 30H). ^{13}C-NMR (500 MHz, $CDCl_3$): δ (ppm) 164.8, 160.5, 151.7, 139.7, 139.2, 132.6, 131.2, 130.1, 125.5, 121.0, 120.0, 118.9, 117.3, 73.1, 55.3, 40.5, 33.4, 31.9, 30.1, 29.8, 29.3, 24.3, 23.9, 22.7, 14.1. FT-IR: 1632 cm^{-1} (C═N), 3434 cm^{-1} (–OH).

Preparation of the test solution for the spectroscopic measurements

For the spectroscopic measurements, solutions of **FSP1**, **FSP2** and **FSP3** (15 μM corresponding to the salen moiety) were prepared in THF separately. Stock solutions of the corresponding cation (2 mM) as its chloride (or in some cases nitrate) salt were prepared in deionized water. All the experiments were carried out by using 2 ml of the particular polymer solution, followed by the addition of aqueous solutions of different metal ions. After the addition of metal ion, the resulting solution was shaken vigorously and the spectra were recorded after 5 min.

Results and discussion

Synthesis and structure of the polymers

The synthesis procedures for the monomer (FSal) and polymers are outlined in Scheme 1. FSal was prepared from 2,7-dibromo-9,9-dioctylfluorene according to our previous report.[9] 2,7-Dibromo-9,9-dioctylfluorene was treated with *n*BuLi at −78 °C in anhydrous tetrahydrofuran, followed by the addition of trimethyl borate to obtain 9,9-dioctylfluorene-2,7-bis(trimethylene boronates) (68%, 1), and it was subsequently reacted with 5-bromosalicylaldehyde in the presence of $Pd(PPh_3)_4$ to obtain FSal (60%). The three fluorene-based salen polymers (**FSP1**, **FSP2**, and **FSP3**) were synthesized from the condensation reaction of FSal and diamine using Schiff-base chemistry according to Scheme 1. The formation of FSal and the three polymers were checked by NMR (Fig. S1–S8, ESI†). The absence of the aldehyde proton at 10.03 ppm in the ^{1}H-NMR spectra and the shift of the aldehyde carbon (196.83 ppm) to ∼164 ppm in the ^{13}C-NMR spectra of the polymer primarily indicate the formation of the polymers. MALDI-TOF revealed the degree of polymerization (DP), which were 9 for all the salen compounds; **FSP1** (MW ∼ 5900, Fig. S9, ESI†), **FSP2** (MW ∼ 6300, Fig. S10, ESI†), and **FSP3** (MW ∼ 6400, Fig. S11, ESI†). FT-IR studies (Fig. S12, ESI†) show the characteristic stretching vibration of C═O at 1709 cm^{-1} and phenolic –OH at 3407 cm^{-1} in FSal. The presence of the stretching vibration of C═N at ∼1634 cm^{-1} and phenolic –OH at ∼3435 cm^{-1} as well as the absence of the stretching vibration of C═O at 1709 cm^{-1} in these derivatives support the formation of fluorene-based salen polymers (**FSP1**, **FSP2**, and **FSP3**).

All three polymers were yellow solid in color, air stable, and highly soluble in common organic solvents like $CHCl_3$, DCM, toluene, THF, *etc.* Among the three fluorene-based salen polymers,

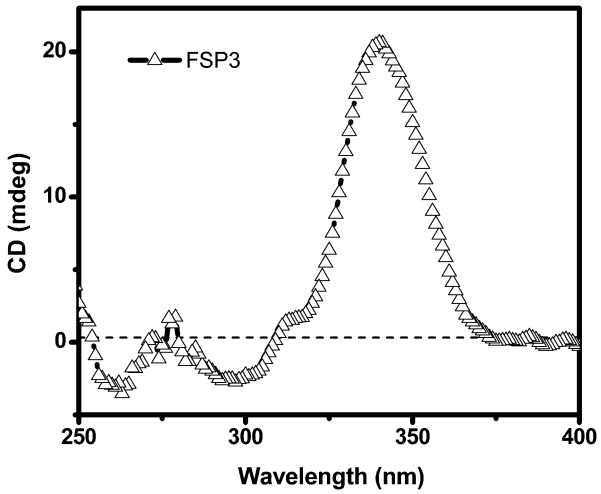

Fig. 1 Circular dichroism spectra of **FSP3** (15 μM) in THF medium.

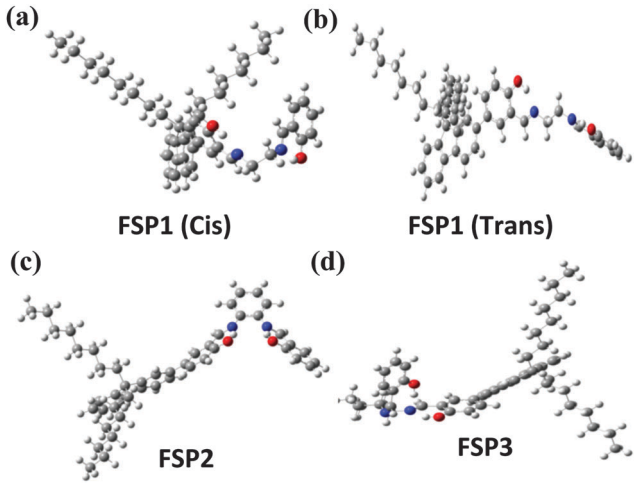

Fig. 2 Energy-minimized structures of the repeating unit of (a) **FSP1** (*cis*-orientation), (b) **FSP1** (*trans*-orientation), (c) **FSP2**, and (d) **FSP3**.

FSP3 was chiral in nature as it was prepared from the reaction between FSal and chiral (1*R*,2*R*)-1,2-diaminocyclohexane. The chiral nature of the **FSP3** was checked by a CD study, which showed a negative and positive cotton effect (Fig. 1) due to the organized helical chain structure of the repeating unit of salen. **FSP3** showed a strong cotton effect at 340 nm, due to its extended conjugated structure.

The thermal stabilities of the salen polymers were relatively high as there was no loss of weight below 350 °C. Two step degradations were seen for all three polymers (Fig. S13, ESI†): in the first step, degradation is observed from 350 °C to 450 °C and probably arises from the degradation of the side chains of polyfluorene. The second degradation is observed from 500 °C to 600 °C and is due to the degradation of the main chain of PF.[30] These polymers have good thermal properties for practical application as fluorescence sensors.

Energy minimization of the repeating unit

To know the orientation four atoms of coordination site of each salen unit present in the main chain of these polymers, geometry optimization has been performed using salen unit of each polymer at the B3LYP/6-31G(d) level and density functional theory (DFT) calculation of three salen units. Sometimes, the salen unit may take in different conformations (*e.g.*, a keto-amine or enol-imine form).[31] The presence of a phenolic proton at ~13.35 ppm in the NMR spectra and the absence of a stretching vibration of C=O at 1709 cm^{-1} (FT-IR) of these three polymers suggest that the enol-imine form of the salen unit is present. Therefore, energy minimization has been performed with the enol-imine form of the polymer. The energy-minimized structure for **FSP1** revealed that the four atoms (ONNO) of the coordination site were not in same plane. Depending on the N–N single bond rotation, **FSP1** may take a *cis*-orientation (four coordination site: ONNO) or a *trans*-orientation (two coordination site: NN)[32] (Fig. 2a and b). The energy-minimized structure of **FSP2** shows that all four atoms of the coordination site are positioned in one plane (Fig. 2c). However in **FSP3**, the orientation of the four atoms of the coordination site is not in a plane (Fig. 2d), rather these four atoms are situated in a distorted tetrahedral fashion. Single-crystal X-ray diffraction structures of different Schiff bases (small molecule) reported in the literature show different orientations of the four atoms of the coordination site.[33] The orientations in the reported crystal structures are very similar with the orientation obtained by the theoretical calculations.

Spectral studies of FSP1

To know how the above orientation of the salen unit affects the binding nature of polymers with different metal ions, we performed optical studies as well as testing the metal sensing ability of **FSP1**, **FSP2**, and **FSP3** with the help of absorption and emission spectroscopic techniques. **FSP1** (15 μM) showed absorption maxima at 334 nm, assigned to π–π* transition (Fig. S14, ESI†). After the addition of 22 equiv. of different metal ions, the absorption maxima of **FSP1** is red-shifted to 4 nm for Fe^{2+}, 24 nm for Cu^{2+}, and 26 nm for Co^{2+} with a higher intensity. Some other metal ions (such as Zn^{2+}, Hg^{2+}, Ag^{+}, and Ni^{2+}) show a red-shifting (~8 nm) of the absorption peak with a lowering of the intensity (Fig. S14, ESI†). Upon excitation at 334 nm, **FSP1** produces very broad and low intensity emission maxima at 530 nm (Fig. 3b). The emission maximum of **FSP1** is shifted to 481 nm for Zn^{2+}, with a 10.5-fold increase in emission intensity. Besides Zn^{2+}, some other metals like Hg^{2+}, Mg^{2+}, Ag^{+}, Sn^{2+}, and Ca^{2+} also show a shifting of the emission peak with a 0.5–4-fold increase in intensity with respect to **FSP1**. A visual bright blue fluorescent color is observed after the addition of Zn^{2+} under a 365 nm UV lamp (Fig. 3a). Alongside Zn^{2+}, other metal ions also produce a blue fluorescent color, except for Co^{2+}, Ni^{2+}, Fe^{2+}, and Cu^{2+} that quench the fluorescence of **FSP1**. As a result, it is difficult to distinguish the visual blue emission color of the **FSP1** + Zn^{2+} complex under a 365 nm UV lamp from the rest of the **FSP1**–metal complexes. This means that **FSP1** does not have selectivity.

Spectral studies of FSP2

The second fluorene-based salen polymer (**FSP2**, 15 μM) showed an absorption peak at 340 nm, which was assigned to

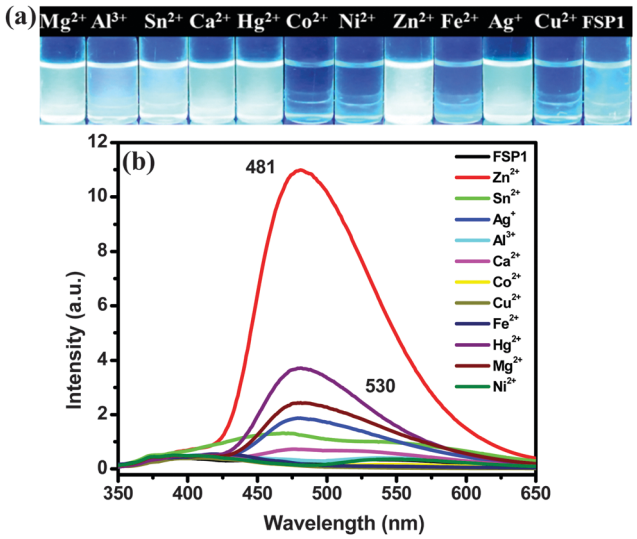

Fig. 3 (a) Fluorogenic response of **FSP1** solution with individual metal ions under a 365 nm UV lamp and (b) emission spectra of **FSP1** (15 μM in THF) upon the addition of different cations (22 equivalents) in H_2O using 334 nm as the excitation wavelength and 5/5 slits.

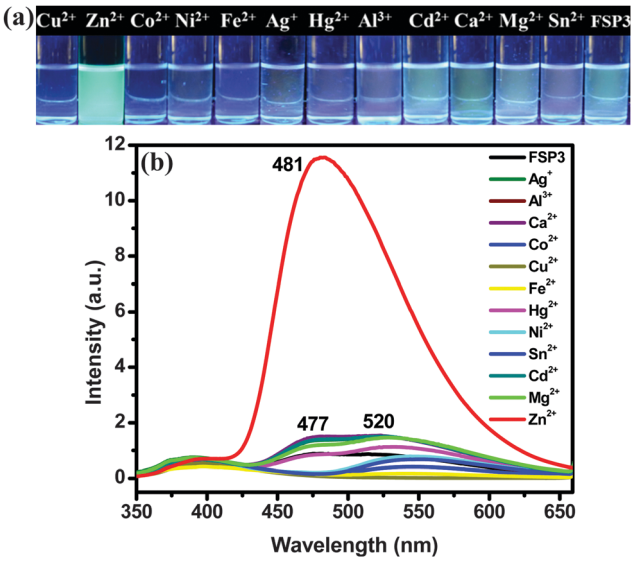

Fig. 5 (a) Fluorogenic response of **FSP3** solution with individual metal ions under a 365 nm UV lamp and (b) emission spectra of **FSP3** (15 μM in THF) upon the addition of different cations (22 equivalents) in H_2O using 333 nm as the excitation wavelength and 5/5 slits.

the π–π* transition of the peak of the polymer. If 22 equiv. of different metal ions (aqueous solution) are added, the absorption peak is red-shifted for Cu^{2+}, Co^{2+}, Fe^{2+}, and Zn^{2+} with a charge transfer band of 400–530 nm (Fig. S15, ESI†).

FSP2 shows two small but broad emission maxima at 500 nm and 588 nm upon excitation at 340 nm. The addition of 22 equiv. of different metal ions to **FSP2** results in the shifting of the emission maximum to a different region in a dissimilar way (Fig. 4b). Titration studies performed with individual metal ions show the affinity of particular metals toward the coordination site (ONNO) of **FSP2** (Fig. S16–S27, ESI†). Upon UV irradiation, a distinct green color is observed with Cu^{2+}, a pink color with Fe^{2+}, and a yellow color with Hg^{2+}, Ag^{+}, Zn^{2+}, Mg^{2+}, and Ca^{2+} ions (Fig. 4a). So **FSP2** is unable to detect any particular metal ion. This does mean that **FSP2** does not have selectivity toward a particular metal ion.

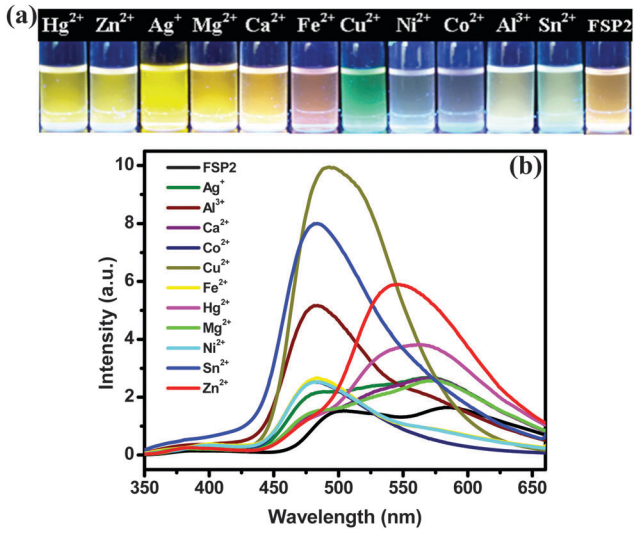

Fig. 4 (a) Fluorogenic response of **FSP2** solution with individual metal ions under a 365 nm UV lamp and (b) emission spectra of **FSP2** (15 μM in THF) upon the addition of different cations (22 equivalents) in H_2O using 340 nm as the excitation wavelength and 5/5 slits.

Spectral studies of FSP3

The third polymer **FSP3**, which is chiral in nature, revealed an absorption peak at 333 nm, attributed to π–π* transition (Fig. S28, ESI†) and a broad emission peak with two shoulders at 477 nm and 520 nm (λ_{ex} = 333 nm) (Fig. 5b). After the addition of 22 equiv. of different metal ions to **FSP3** solution, we did not observe a charge transfer band for any metal ion. Whereas, the emission peak of **FSP3** was remarkably blue-shifted from 520 to 481 nm with a substantial increase (11.5-fold) in the emission intensity only for Zn^{2+}. Also a visual bright blue fluorescent color was observed for Zn^{2+} under UV light (Fig. 5a), indicating that **FSP3** is a highly selective fluorescence sensor for Zn^{2+} ions only. To check for interference from Cd^{2+} ions, fluorescence studies of **FSP3** were carried out with Cd^{2+} and no effect of Cd^{2+} toward **FSP3** (Fig. 5b) was observed. Therefore, **FSP3** is a promising candidate and could be used as a fluorescent sensor for selective Zn^{2+} ion detection.

Fluorometric titration of FSP3 with Zn^{2+} ions

A titration experiment was performed by taking **FSP3** (15 μM in THF) with the continuous addition of Zn^{2+} solution (Fig. 6a), and the fluorescent intensity of **FSP3** at 481 nm was gradually increased up to 22 equiv. of Zn^{2+} ion addition. A plot of $I/I_0 - 1$ (where I_0 is the intensity of **FSP3** at 520 nm and I is the intensity at 481 nm for the **FSP3** + Zn^{2+} complex) against $[Zn^{2+}]$ maintained a linear correlation up to 15 equiv. of metal ions (inset of Fig. 6a). From that curve, a detection limit was found to be 50 μM (Fig. S29, ESI†). The fluorescence response by individual metal ions

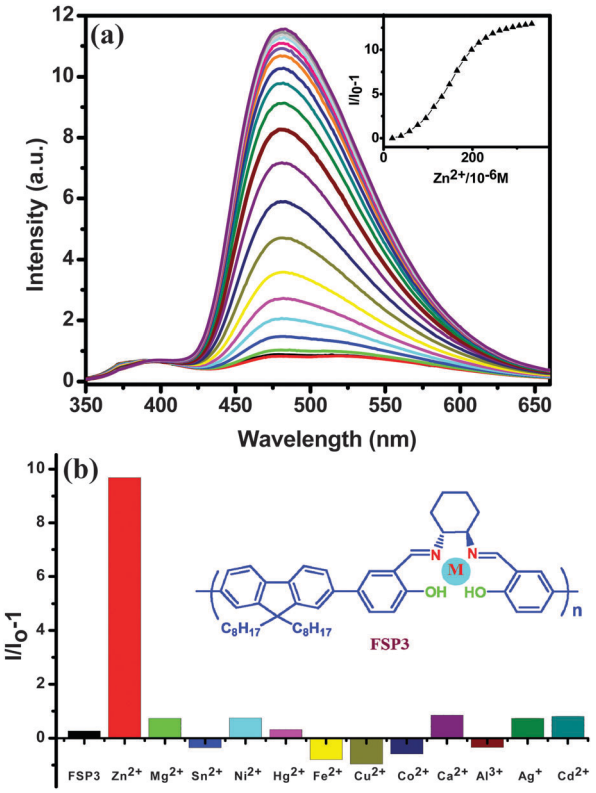

Fig. 6 (a) Fluorescence titration spectra of **FSP3** (15 μM in THF) with the continuous addition of Zn^{2+} up to 22 equiv. in water (inset figure: plot of I/I_0 1 *vs.* [Zn^{2+}]) and (b) bar plot showing the fluorescence response of **FSP3** in the presence of different metal ions. The metal binding sites in each salen unit are shown in the inset.

was demonstrated by a representative bar plot (Fig. 6b). Among the metal ions, Fe^{2+}, Cu^{2+}, and Co^{2+} more or less completely quench the fluorescence, whereas Sn^{2+} and Al^{3+} quench the fluorescence of **FSP3** only limitedly. Binding constants for metal ions were calculated using Benesi–Hildebrand's equation.[34] The binding constant for Zn^{2+} is 2.57 × 10^4 M^{-1}. The selectivity of **FSP3** toward Zn^{2+} in the presence of other cations was also checked (Fig. S30, ESI†). The fluorescence intensities remained unaltered in the presence of excess other cations, except for the coexisting ions (Fe^{2+}, Co^{2+} and Cu^{2+}) that showed interference to a small extent. Also, upon the gradual addition of Zn^{2+} to the solution of **FSP3**, the CD intensity diminished (Fig. S31, ESI†), showing the formation of a **FSP3** + Zn^{2+} complex.

Mechanism

Resulting from all the above studies, we concluded that **FSP1** and **FSP2** have no selectivity for any particular metal ion. However, **FSP3** is highly selective and sensitive to Zn^{2+} ions. It detects Zn^{2+} ions through turn-on fluorescence. This turn-on fluorescence is possibly due to the suppressed PET quenching when the metal ion coordinates with the nitrogen atom of the salen moieties. After complexation, the lone pair of electrons on the nitrogen atom is no longer available for PET, leading to the enhancement of fluorescence.[35] In addition; metal ion detection is obviously associated with the fluorescence enhancement with a blue-shifting of the emission maxima. This blue-shifting may be attributed to the decrease in energy of the HOMO of the conjugated part of the salen polymer.[36] As all three polymers (**FSP1**, **FSP2**, and **FSP3**) contain same coordination sites (ONNO), they should bind the same metal ions. In reality, we obtained different results. **FSP1** and **FSP2** had no selectivity. However, **FSP3** was highly selective toward Zn^{2+} ions. This anomalous behavior can be explained by considering the orientation of the four atoms of the coordination site into the long chain polymer. The four atoms of the coordination site in **FSP1** are not in a plane, as two N atoms are connected through a flexible single bond. In **FSP2**, the four atoms of the coordination site are nearly close to remaining in a plane as they are connected through a planar benzene ring. In **FSP3**, the four atoms of the coordination site are not in a plane and N–N bond rotation is not allowed, owing to the presence of a rigid cyclohexane system, which is connected in between two N atoms. Thus, the orientation of the coordination site differs from polymer to polymer.

From basic crystal field theory, we know that Zn^{2+} ions ($3d^{10}$) have a tendency to form tetrahedral complexes rather than square-planar complexes. In **FSP3**, the non-planarity of the coordination sites in a nearly tetrahedral fashion makes it more selective for Zn^{2+} ions than any other metal ions. However, in **FSP1** and **FSP2** the orientation of the coordination sites does not allow suitable tetrahedral binding mode to detect Zn^{2+}. The energy-minimized structure of **FSP3** + Zn^{2+} complex shows that Zn^{2+} is nicely fitted in a distorted tetrahedral geometry in the cavity of the coordination site of **FSP3**. We estimated the bond length and bond angles of the monomeric unit of the **FSP3** + Zn^{2+} complex. These are 1.922 Å/2.084 Å (Zn–N) and 1.976 Å /2.084 Å (Zn–O) (Fig. S32, ESI†). To find out about the nature of charge transfer into this polymer and polymer–metal complex, TD-DFT calculations of **FSP3** and the **FSP3** + Zn^{2+} complex were performed. The UV-Vis study of FSP3 showed the absorption maximum at 333 nm. From the TD-DFT calculation, the estimated absorption maximum of **FSP3** is 309 nm (π–π* transition (HOMO → LUMO+1)) with an oscillator strength f = 0.7749, (Fig. 7a and Fig. S33, ESI†), and in **FSP3** + Zn^{2+} complex the peak at 352 nm corresponds to HOMO → LUMO+5 transition with an oscillator strength f = 0.3798 (Fig. 7b and Fig. S34, ESI†).

To support the above theoretical explanation, we performed the ^{1}H-NMR titration of **FSP1–FSP3** with Zn^{2+} ions and 2D NMR to find out about the coordination geometry (see ESI† for details of the NMR study, Fig. S35–S37). ^{1}H-NMR titration of the polymers with Zn^{2+} indicated that all the polymers bind Zn^{2+} ions. Upon binding, the –OH and –N=C–H proton are shifted to a higher field, which supports the binding of Zn^{2+} with the four coordinating donor atoms (ONNO). In order to find out the coordination geometry, we also assigned all the signals of the ^{1}H-NMR of **FSP2** and **FSP3** with the help of COSY and NOESY NMR studies (Fig S38 and S39, ESI†) of the corresponding salen polymers. The NOESY spectra of **FSP2** (shown in the colored box in Fig. S40, ESI†) demonstrated only one major interaction of H_b proton with H_d. However, the

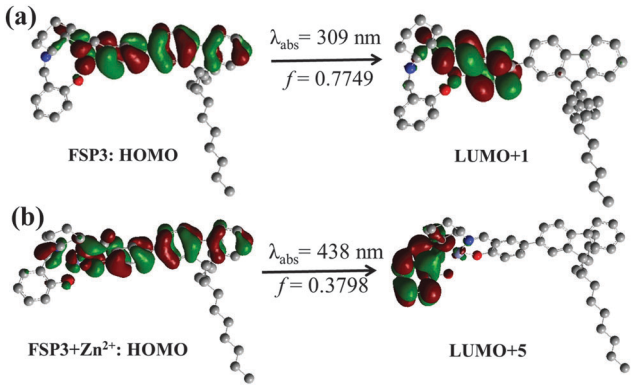

Fig. 7 (a) HOMO and LUMO+1 of **FSP3** (b) HOMO and LUMO+5 of **FSP3** + Zn^{2+} complex.

NOESY spectra of **FSP3** revealed many major interactions, such as, H_b–H_c, H_b–H_d, H_b–H_e, H_b–H_g, H_b–H_f, H_f–H_d, and H_k–H_d, *etc.* (shown in the colored boxes in Fig. S41, ESI†). As H_b protons in **FSP3** have exhibited many interactions with the proton of the appended cyclohexane moiety and fluorene moiety, this indicated the non-planner geometry of the four atoms of the coordination site of **FSP3**, which mean that there is a distorted tetrahedral geometry in the cavity of the coordination site of **FSP3**. In **FSP2**, H_b protons showed less interaction with other protons due to the rigid planner structure to provide square planner geometry of the coordination sites.

Conclusions

In summary, three different fluorene-based $(A–B)_n$-type salen polymers (**FSP1**, **FSP2**, and **FSP3**) were synthesized and characterized with the help of NMR and MALDI-TOF. Among these, two (**FSP1** and **FSP2**) were achiral, while **FSP3** was chiral in nature, as confirmed by a CD study. The selectivity of these polymers toward metal ions was studied with the help of absorption and emission studies. **FSP1** and **FSP2** had no selectivity for any metal ions, whereas **FSP3** showed high sensitivity and selectivity toward Zn^{2+} ions by a florescence 'turn-on' mechanism. This phenomenon of selective metal ion binding through fluorescence enhancement is not only the effect of PET but there is another significant effect, *i.e.*, the effect of the orientation of the four atoms of the coordination sites (*i.e.*, the orientation effect). **FSP3** binds with the metal ion in a specific geometry that is ultimately reflected through the selectivity. This phenomenon was overwhelmingly supported by theoretical calculation. This also helps to explain the nature of charge transport into the polymer and the polymer–metal ion complex. Further we examined the coordination geometry with the help of 2D NMR spectra. The present study opens the door to the design of novel kinds of sensor systems, metallo-polymers, and their applications.

Acknowledgements

M.K.B. acknowledges CSIR for the financial support. M.K.B. also acknowledges to Mr Chandan Sahu, IACS for his valuable assistance and discussions.

References

1 J. F. Callan, A. P. De Silva and D. C. Magri, *Tetrahedron*, 2005, **61**, 8551.
2 A. W. Czarnik, *Acc. Chem. Res.*, 1994, **27**, 302.
3 H. Schiff, *Ann. Chem.*, 1864, **3**, 343.
4 F. A. Carey, *Organic chemistry*, McGraw-Hill, New York, 5th edn, 2003, p. 724.
5 P. G. Lacroix, *Eur. J. Inorg. Chem.*, 2001, 339.
6 P. G. Cozzi, *Chem. Soc. Rev.*, 2004, **33**, 410.
7 F. Thomas, O. Jarjayes, C. Duboc, C. Philouze, E. Saint-Aman and J. Louis Pierre, *Dalton Trans.*, 2004, 2662.
8 X. Xu, C. S. Allen, C. L. Chuang and J. W. Canary, *Acta Crystallogr.*, 1998, **54**, 600.
9 M. K. Bera, C. Chakraborty, P. K. Singh, C. Sahu, K. Sen, S. Maji, A. K. Das and S. Malik, *J. Mater. Chem. B*, 2014, **2**, 4733.
10 A. I. Bush, *Curr. Opin. Chem. Biol.*, 2000, **4**, 184.
11 A. I. Bush, *Trends Neurosci.*, 2003, **26**, 207.
12 M. B. Sorensen, M. Stoltenberg, S. Juhl, G. Danscher and E. Ernst, *Prostate*, 1997, **31**, 125.
13 A. B. Chausmer, *J. Am. Coll. Nutr.*, 1998, **17**, 109.
14 S. C. Burdette, G. K. Walkup, B. Spingler, R. Y. Tsien and S. J. Lippard, *J. Am. Chem. Soc.*, 2001, **123**, 7831.
15 P. J. Jiang, L. Z. Chen, J. Lin, Q. Liu, J. Ding, X. Gao and Z. J. Guo, *Chem. Commun.*, 2002, 1424.
16 H. Wang, Q. Gan, X. Wang, L. Xue, S. Liu and H. Jiang, *Org. Lett.*, 2007, **9**, 4995.
17 M. D. Shults, D. A. Pearce and B. Imperiali, *J. Am. Chem. Soc.*, 2003, **125**, 10591.
18 S. He, S. T. Iacono, S. M. Budy, A. E. Dennis, D. W. Smith Jr and R. C. Smith, *J. Mater. Chem.*, 2008, **18**, 1970.
19 R. P. Kingsborough and T. M. Swager, *J. Am. Chem. Soc.*, 1999, **121**, 8825.
20 D. T. McQuade, A. E. Pullen and T. M. Swager, *Chem. Rev.*, 2000, **100**, 2537.
21 S. W. Thomas, G. D. Joly and T. M. Swager, *Chem. Rev.*, 2007, **107**, 1339.
22 Y. Xu, J. Meng, L. X. Meng, Y. Dong, Y. X. Cheng and C. J. Zhu, *Chem. – Eur. J.*, 2010, **16**, 12898.
23 F. Y. Song, X. Ma, J. L. Hou, X. B. Huang, Y. X. Cheng and C. J. Zhu, *Polymer*, 2011, **52**, 6029.
24 Y. Dong, Y. Wu, X. Jiang, X. Huang, Y. Cheng and C. Zhu, *Polymer*, 2011, **52**, 5811.
25 J.-F. Li, Y.-Z. Wu, F.-Y. Song, G. Wei, Y.-X. Cheng and C.-J. Zhu, *J. Mater. Chem.*, 2012, **22**, 478.
26 M. J. Frisch, G. W. Trucks, H. B. Schlegel, G. E. Scuseria, M. A. Robb, J. R. Cheeseman, G. Scalmani, V. Barone, B. Mennucci and G. A. Petersson, *et al.*, *Gaussian 09, rev. B.01*, Gaussian, Inc., Wallingford CT, 2009.
27 A. D. Becke, *Phys. Rev. A: At., Mol., Opt. Phys.*, 1988, **38**, 3098.
28 C. Lee, W. Yang and R. G. Parr, *Phys. Rev. B: Condens. Matter Mater. Phys.*, 1988, **37**, 785.
29 O. Treutler and R. J. Ahlrichs, *Chem. Phys.*, 1995, **102**, 346.
30 C. Chakraborty, K. Dana and S. Malik, *J. Colloid Interface Sci.*, 2012, **368**, 172.

31 V. Z. Mota, D. G. S. G. Carvalho, P. P. Corbi, F. R. G. Bergamini, A. L. B. Formiga, R. Diniz, M. C. R. Freitas, A. D. Da Silva and A. Cuin, *Spectrochim. Acta, Part A*, 2012, **99**, 110.
32 C. Diaz, A. Frazer, A. Morales, K. D. Belfield, S. Ray and F. E. Hernandez, *J. Phys. Chem. A*, 2012, **116**, 2453.
33 L. Zhou, Y. Feng, J. Cheng, N. Sun, X. Zhou and H. Xiang, *RSC Adv.*, 2012, **2**, 10529.
34 V. K. Indirapriyadharshini, P. Karunanithi and P. Ramamurthy, *Langmuir*, 2001, **17**, 4056.
35 Z. C. Xu, K. H. Baek, H. N. Kim, J. N. Cui, X. H. Qian, D. R. Spring, I. J. Shin and J. Y. Yoon, *J. Am. Chem. Soc.*, 2010, **132**, 601.
36 Y. W. Wang, M. X. Yu, Y. H. Yu, Z. P. Bai, Z. Shen, F. Y. Li and X. Z. You, *Tetrahedron Lett.*, 2009, **50**, 6169.

